

1 Technical Note: Noble gas extraction procedure and performance of the  
2 Cologne Helix MC Plus multi-collector noble gas mass spectrometer for  
3 cosmogenic neon isotope analysis

4 Benedikt Ritter<sup>1\*</sup>, Andreas Vogt<sup>1</sup>, Tibor J. Dunai<sup>1\*</sup>

5 <sup>1</sup> University of Cologne, Institute of Geology and Mineralogy, Zùlpicher StraÙe 49b, Köln 50674,  
6 Germany

7 \*Corresponding authors

8 Benedikt Ritter – [benedikt.ritter@uni-koeln.de](mailto:benedikt.ritter@uni-koeln.de)

9 Tibor J. Dunai – [tdunai@uni-koeln.de](mailto:tdunai@uni-koeln.de)

10 Keywords: Noble Gas, Mass Spectrometry, Cosmogenic Nuclides

11  
12 **Abstract:**

13 We established a new laboratory for noble gas mass spectrometry that is dedicated to the  
14 development and application to cosmogenic nuclides at the University of Cologne (Germany). At  
15 the core of the laboratory are a state-of-the-art high mass resolution multicollector Helix MCPlus  
16 (Thermo-Fisher) noble gas mass spectrometer and a novel custom-designed automated  
17 extraction line. The mass spectrometer is equipped with five combined Faraday Multiplier  
18 collectors, with  $10^{12} \Omega$  and  $10^{13} \Omega$  pre-amplifiers for faraday collectors. We describe the extraction  
19 line and the automated procedure for cosmogenic neon and the current performance of the  
20 experimental setup. Performance tests were conducted using gas of atmospheric isotopic  
21 composition (our primary standard gas), as well as CREU-1 intercomparison material, containing  
22 a mixture of neon of atmospheric and cosmogenic composition. We use the results from repeated  
23 analysis of CREU-1 to assess the performance of the current experimental setup at Cologne. The  
24 precision in determining the abundance of cosmogenic  $^{21}\text{Ne}$  is equal to or better than those  
25 reported for other laboratories. The absolute value we obtain for the concentration of cosmogenic  
26  $^{21}\text{Ne}$  in CREU is indistinguishable from the published value.

27 **1. Introduction**

28 Cosmogenic Ne isotopes are stable and compared to other cosmogenic radionuclides (e.g.,  $^{10}\text{Be}$ ,  
29  $^{26}\text{Al}$ ) exhibit the potential to date beyond the physical limit of radionuclides. The particular  
30 strength of cosmogenic neon is its application to date quartz clasts of very old surfaces (>4 Ma) or  
31 very slowly eroding landscapes (<10 cm/Ma), which is unattainable with most other  
32 radionuclides (Dunai, 2010). Cosmogenic Ne analysis can be applied to a range of neon-retentive  
33 minerals (e.g., quartz, olivine and pyroxene), amongst which quartz is the most commonly used.  
34 Ne can be measured on conventional sector field noble gas mass spectrometers, is less time  
35 consuming and requires less sample-preparation compared to AMS measurements required for

36 the cosmogenic radionuclides. Recent studies used cosmogenic Ne for dating old surfaces (e.g.  
37 Ritter et al., 2018; Dunai et al., 2005; Binnie et al., 2020), reconstructing erosion rates (e.g. Ma et  
38 al., 2016), or  $^{10}\text{Be}/^{21}\text{Ne}$  burial dating (e.g. McPhillips et al., 2016). The advantage to use also other  
39 minerals than quartz, led to several studies using  $^{21}\text{Ne}$  to date for example basalt flows (e.g.  
40 Espanon et al., 2014; Gillen et al., 2010). Neon has three stable isotopes  $^{20}\text{Ne}$ ,  $^{21}\text{Ne}$ , and  $^{22}\text{Ne}$ , of  
41 which  $^{20}\text{Ne}$  is the most abundant; the atmospheric  $^{21}\text{Ne}/^{20}\text{Ne}$  and  $^{22}\text{Ne}/^{20}\text{Ne}$  ratios are  $0.002959 \pm$   
42  $0.000022$  and  $0.1020 \pm 0.0008$ , respectively (Eberhardt et al., 1965). There are several recent  
43 re-determinations of the atmospheric  $^{21}\text{Ne}/^{20}\text{Ne}$  ratio (e.g. Honda et al., 2015; Wielandt and  
44 Storey, 2019; Saxton, 2020; Györe et al., 2019) one of which yields a  $\sim 2\%$  lower value (Honda et  
45 al., 2015). For the evaluation of our data, we utilize the  $^{21}\text{Ne}/^{20}\text{Ne}$  value of Wielandt and Storey  
46 (2019) of  $0.0029577 \pm 0.0000014$  and for  $^{22}\text{Ne}/^{20}\text{Ne}$  that of Eberhardt et al. (1965). Note, that in  
47 the context of the determination of the *abundance* of cosmogenic nuclides in a sample eventual  
48 differences between the used and the actual value of the atmospheric  $^{21}\text{Ne}/^{20}\text{Ne}$  ratio are  
49 unimportant, if (i) atmospheric neon is used as calibration gas, (ii) the same value for the  
50 composition of atmospheric neon is used consistently throughout the evaluation of the isotope  
51 data (mass discrimination etc.) and calculation of abundances and (iii) the atmospheric value used  
52 is reported along with the data.

53 All three neon isotopes are produced in about equal proportions by neutron spallation in quartz  
54 (Niedermann et al., 1994). Due to the lower abundances of  $^{21}\text{Ne}$  and  $^{22}\text{Ne}$  as compared to  $^{20}\text{Ne}$  in  
55 air, and the ubiquitous presence of atmospheric neon in samples, any contribution from  
56 cosmogenic production in samples is most easily picked up with the former two isotopes.  
57 Consequently, the neon three-isotope diagram with  $^{20}\text{Ne}$  as common denominator (Niedermann  
58 et al., 1994; Niedermann, 2002) is customarily used to assess  $^{21}\text{Ne}$ -data for the presence of  
59 terrestrial cosmogenic Ne and its discrimination from other non-atmospheric Ne-components  
60 (Dunai, 2010). The latter may be nucleonic Ne and/or mantle-derived Ne. Hence, the accurate  
61 determination of cosmogenic Ne and its discrimination from other components requires the  
62 accurate discrimination from any other component.

63 **Common isobaric interferences for neon measurements are at:  $m/e = 20$  ( $^{40}\text{Ar}^{2+}$ ,  $\text{H}^{19}\text{F}^+$  and  $\text{H}_2^{18}\text{O}^+$   
64 **interfering with  $^{20}\text{Ne}^+$** ), at  $m/e = 21$  ( $^{20}\text{NeH}^+$ , interfering with  $^{21}\text{Ne}^+$ ), and at  $m/e = 22$  ( $^{44}\text{CO}_2^{2+}$   
65 **interfering with  $^{22}\text{Ne}^+$** ).**  $^{40}\text{Ar}^{2+}$  and  $^{12}\text{C}^{16}\text{O}_2^{2+}$  interferences are considered to be the main challenges  
66 for neon analysis. Recent studies demonstrated the ability of the Helix MCPlus to fully resolve the  
67  $^{40}\text{Ar}^{2+}$ ,  $\text{H}^{19}\text{F}^+$  and  $\text{H}_2^{18}\text{O}^+$  peaks from the  $^{20}\text{Ne}^+$  peak (e.g. Honda et al., 2015; Wielandt and Storey,  
68 2019) and its ability to reliably measure  $^{21}\text{Ne}$  at an off-centre peak position that is free of  
69 interference from  $^{20}\text{NeH}^+$  (Honda et al., 2015; Wielandt and Storey, 2019). The remaining  
70 interference of  $^{12}\text{C}^{16}\text{O}_2^{2+}$  at  $m/e = 22$  can be corrected via monitoring of the double/single-charged  
71 ratio of  $\text{CO}_2$  in-between samples (Honda et al., 2015) or the measurement of  $^{13}\text{C}^{16}\text{O}_2^{2+}$  at

72 m/e = 22.5 during sample analysis (Wielandt and Storey, 2019). Recently mass spectrometers  
73 with higher resolution have become available, which permit almost full separation of  $^{12}\text{C}^{16}\text{O}_2^{2+}$  and  
74  $^{22}\text{Ne}$  (Farley et al., 2020).

75 Beside the resolution and characteristics of a noble gas mass spectrometer to resolve and  
76 quantitatively determine neon compositions of an unknown sample, the calibration, sample  
77 extraction and purification are crucial achieving accurate and reproducible results. Automation of  
78 extraction protocols and workflows may assist in achieving a high degree of reproducibility by  
79 eliminating inaccuracies or errors by operators having a variable degree of expertise. In this  
80 paper, we describe the current setup of the noble gas mass spectrometer and its automated  
81 extraction line that is located in the Institute of Geology and Mineralogy at the University of  
82 Cologne (Germany), and we review its performance for neon analysis.

## 83 **2. Experimental setup**

### 84 **2.1 Noble gas mass-spectrometer**

85 The Cologne noble gas laboratory is equipped with a Helix MCPlus from Thermo Fisher Scientific  
86 with five CFM modules (Combined Faraday Multiplier), called 'Aura'. The central, axial module  
87 (Ax) is fixed in position, the four remaining modules (L1, L2 on the low mass side, and H1,  
88 H2 on the high mass side of Ax) can be moved. The mass spectrometer configuration and  
89 performance is mostly equivalent to those described elsewhere (Honda et al., 2015; Wielandt and  
90 Storey, 2019); here we describe potential differences in configuration and performance  
91 parameters that may be unique to a given instrument (Fig. 1).

92 In the instrument at Cologne University, all but one Faraday amplifier, are equipped with  $10^{13} \Omega$   
93 resistors, one with  $10^{12} \Omega$  (H2). The L1 module has 0.3 mm wide collector slits, all other modules  
94 have 0.6 mm wide slits. The CFM at L1 configuration is flipped (i.e., the relative positions of the  
95 Faraday and Multiplier are swapped) as compared to the standard configuration, which is the only  
96 difference from the standard configuration. The two SAES NP10 getters, at the source and the  
97 multiplier block, are kept at room temperature during analysis.

98 For neon isotope analysis of calibrations and samples, we utilize the H1, Ax and L1 CFMs ( $^{20}\text{Ne}^+$   
99 L1 Faraday;  $^{22}\text{Ne}^+$  H1 Faraday;  $^{21}\text{Ne}^+$  L1 multiplier;  $\text{CO}_2^+$  H1 Faraday; for blanks we utilize the L1  
100 multiplier also for  $^{20}\text{Ne}^+$  and  $^{22}\text{Ne}^{++}$ ). With the widest source slit (0.25 mm) mass resolution (at 5%  
101 peak valley) and mass resolving power (between 10% and 90% of peak) on the L1 detector with  
102 0.3 mm collector slit width are approximately 1700 and 6500, respectively. For the Ax and H1  
103 detectors with 0.6 mm collector slit, the corresponding values are approximately 1000 and 6000,  
104 respectively. As such the system allows the interference-free determination of  $^{20}\text{Ne}$  and  $^{21}\text{Ne}$ ; for

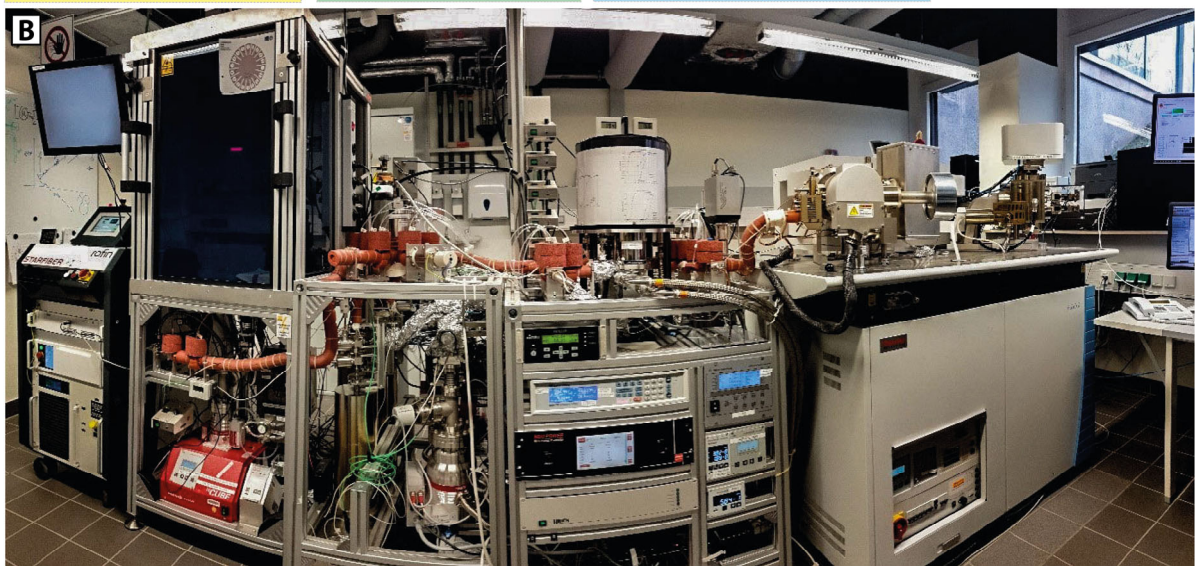
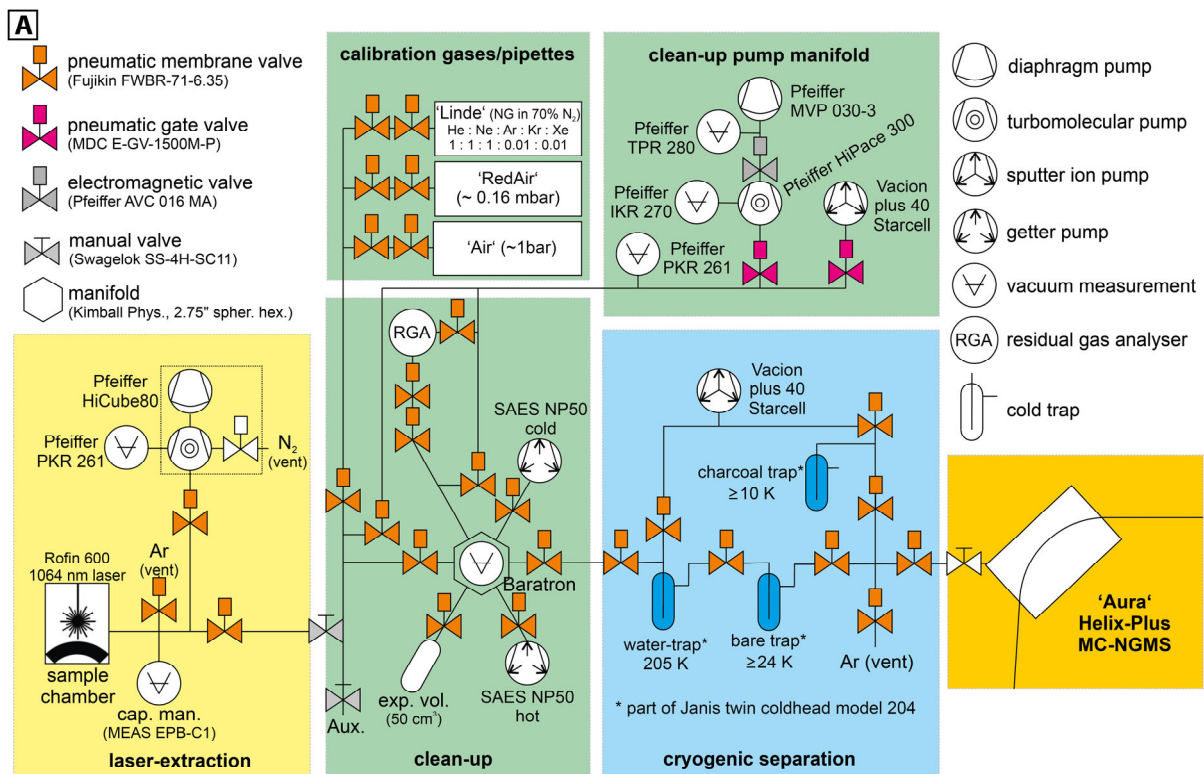
105 <sup>21</sup>Ne this entails measuring at an off-centre peak position (Honda et al., 2015; Wielandt and Storey,  
106 2019).

## 107 **2.2 Extraction line**

108 The **Cologne** noble gas extraction and purification line has a modular design (**Fig. 1**). Modules are  
109 (i) extraction (currently only laser extraction; to be joined by a crushing device), (ii) calibration  
110 gas pipettes and volumes, (iii) clean-up, and (iv) cryogenic separation. The calibration module is  
111 physically linked to the clean-up module, the other modules can be separated, if required. Among  
112 the common features of all modules is that all valves and tubing in contact with the sample gas are  
113 made of metal; tubing is of stainless steel or vacuum-annealed copper. Furthermore, all valves  
114 used for handling of sample and calibration gas are pneumatically actuated all-metal diaphragm  
115 valves (Fujikin MEGA-M LA; FWB(R)-71-6.35), that can be operated at high temperature (up to  
116 350°C). Tubing and valves in contact with sample gas are continuously kept at constant  
117 temperature between 160 °C and 200 °C; exceptions are the functional traps and portions of the  
118 tubing in the cryogenic separation. Temperature is maintained with heating tapes (Horst HS  
119 450 °C) and is controlled section-wise (Horst HT30). The temperature of the heated sections is  
120 controlled to ±1 °C. Thermal insulation is achieved with high-temperature resistant silicone foam  
121 (HOKOSIL®; resists ≤280 °C; permitting bake-out at higher than operation temperatures).  
122 Vacuum connections used are VCR (for Fujikin Valves), CF (for adapters, getters and manifold in  
123 clean up) and Swagelok (for flexible tubing between modules and between ports of the cryogenic  
124 separator (Swagelok 321 Stainless Steel Flexible Tubing with XBA adapter; and copper tubing).  
125 Tubing and valves are 1/4" outer diameter (Swagelok) or equivalent (VCR, Fujikin). The overall  
126 internal volume of the extraction line (laser-extraction, clean-up & cryogenic separation) is  
127 530 cm<sup>3</sup>. Outside the volume used for sample preparation, CF connections are used throughout. A  
128 schematic overview and picture of the extraction line is provided in **Figure 1**.

129

130



131

132 *Fig. 1: (A) Schematic plan and picture (B) of the noble gas extraction and purification line at the*  
 133 *University of Cologne. From left to right: Rofin Starfiber 600, full-protection laser-cage (laser*  
 134 *protection windows P1P10, Laservision) housing the laser extraction, clean up unit, cryogenic*  
 135 *separation unit and the Helix Plus NG-MCMS 'Aura'. The laboratory is temperature-stabilized to*  
 136 *±0.5 °C. Further description is provided in the text.*

137 More specifically about the individual modules:

- 138 i. Laser extraction module (Fig. 1): Up to eighteen tungsten cups are loaded in a sample revolver,  
 139 housed in a DN 200 CF flange-sandwich. The sample revolver is machined from molybdenum,  
 140 which permits the heating of the tungsten cups while being situated in the revolver. To

141 minimize heat-loss through conduction, the cups sit on shards of zirconia (synthetic, cubic-  
142 stabilized  $ZrO_2$ ). The tungsten cups can hold up to ~600 mg quartz. The tungsten cups are  
143 reused. When analysing quartz, tungsten cups are emptied with a suction micropicker  
144 (Micropicker MPC100; VU Amsterdam), while remaining in the sample revolver. In cases  
145 where samples are melted during extraction, tungsten cups could be cleaned in HF (then of  
146 course outside the revolver). For sample loading the volume containing the revolver is vented  
147 and continuously flushed with high-purity nitrogen. During laser extraction the pressure is  
148 monitored (MEAS EPB-C1 sensor, welded into a male VCR connector; Disynet), in case of an  
149 eventual failure of the viewport, the extraction volume is automatically purged with Argon.  
150 Energy for the heat-extraction is provided by an output-tuneable 600 W fiberlaser (Rofin  
151 StarFiber600) at 1064 nm wavelength through galvanometer scanner optics (Rofin RS S 14  
152 163/67 0°) and a sapphire viewport (Kurt Lesker, VPZL-275DUS). For neon-extraction of  
153 quartz, the cups are covered with tungsten-lids; the heating occurs via scanning of the lids  
154 (scanning speed 20 cm/s; rastering a circular area of 10 mm diameter) with a defocused (~  
155 0.5 mm diameter) continuous wave beam with 100 W power for 15 min. Copper (melting point  
156 1085 °C), placed in the cup-assemblies, melts at 80 W laser power (15 min extraction time);  
157 we assume that at 100 W laser power the internal temperature is  $\geq 1200$  °C. The temperature  
158 of the top of the tungsten lids is monitored with a pyrometer (CellaTemp PA 29 AF 2/L; Keller  
159 HCW). The laser extraction has a dedicated pumping unit (Pfeiffer HiCube80). Pressures  
160 attained after sample loading and heating of the revolver (via short-term laser-heating -  
161 stepwise increased to 200 W - of an empty tungsten cup; the external housing flanges reach  
162 ~50 °C during this treatment; temperatures in adjacent cups in the revolver stay below  
163 156.6° C, which was verified with Indium wire) are usually  $< 5 \times 10^{-9}$  mbar (the lower limit of  
164 the pressure gauge used) after one night of pumping. Typical blanks, obtained via heating of  
165 an empty tungsten cup assembly, are ~0.3 fmo| Neon. A detailed description of this novel  
166 laser-furnace will be provided elsewhere.

167 ii. Calibration gas pipette module (Fig. 1): The gas-pipettes are assemblies of male and female  
168 versions of pneumatically actuated Fujikin diaphragm valves (MEGA-M LA; FWB(R)-71-6.35);  
169 the reservoirs were manufactured by Caburn-MDC, the insides of the reservoirs are  
170 electropolished. We currently have three different gases available for noble gas calibration  
171 ('Linde', 'Air', 'RedAir'). 'Linde' is a noble gas mixture in nitrogen ( $9.889 \pm 0.009\%$  He,  
172  $10.00 \pm 0.01\%$  Ne,  $10.01 \pm 0.01\%$  Ar,  $0.00987 \pm 0.0003\%$  Kr;  $0.01023 \pm 0.00002\%$  Xe; all  
173 uncertainties are  $\pm 2\sigma$ ; remainder  $N_2$ , prepared gravimetrically by Linde; values as certified by  
174 Linde according to DIN ISO 6141) the He is enriched in  $^3He$  ( $12.3 \pm 0.3 R_a$ ;  $\pm 2\sigma$ ; value as certified  
175 by Linde according to DIN ISO 6141), the remaining noble gases have atmospheric  
176 composition. We assume that the cryogenically purified atmospheric gases used by Linde were

177 not fractionated during this process; we have verified this for Ne within the limits of  
178 uncertainties reported in this paper. 'Air' is a reservoir of air at atmospheric pressure and  
179 'RedAir' a reservoir of air at reduced pressure (lab-name 'RedAir' is the abbreviation of that  
180 fact). For the neon determinations we utilize 'RedAir'. The volumes of all reservoirs and the  
181 pipettes have been determined relative to a gravimetrically calibrated gas volume (an  
182 assembly of a Swagelok SS-4H valve and a Swagelok SS-4CS-TW-50 miniature cylinder;  
183 repeatedly weighed (Satorius MSA524P-1000-DI; the balance was calibrated prior to  
184 calibration of the reference volume) under vacuum and filled with air at a temperature (n=16),  
185 pressure and relative humidity measured with traceable and/or certified sensors  
186 (thermometer: testo 110; manometer: Greisinger GMH 3181-12, DKD certificate D19853, D-K-  
187 15070-01-01; hygrometer: VWR traceable 628-0031); reference volume is  $51.37 \pm 0.18 \text{ cm}^3$   
188 ( $\pm 1\sigma$ ). All other volumes (piping of the calibration gas filling line; pipettes and reservoirs) were  
189 determined by taking pressure readings (MKS Baratron, Type 628FU5TCF1B) from repeated  
190 step-wise expansion of gases. The temperature in the room where these calibrations were  
191 conducted was stable to  $\pm 0.5 \text{ }^\circ\text{C}$  over the course of the calibrations. The thus determined  
192 volumes of the reservoir and pipette of 'RedAir' are  $8740 \pm 35 \text{ cm}^3$  and  $1.457 \pm 0.006 \text{ cm}^3$  ( $\pm 1\sigma$ ),  
193 respectively. For filling of the 'RedAir' reservoir one pipette volume of air was expanded into  
194 the reservoir; the temperature, pressure and humidity at the time of filling of the pipette were  
195 measured with a traceable and certified sensor (same as above). The first pipette volume  
196 extracted from the 'RedAir' reservoir contained  $4.020 \pm 0.027 \times 10^{-9} \text{ cm}^3$  ( $\pm 1\sigma$ ) atmospheric  
197 neon at standard temperature and pressure ( $179 \pm 1 \text{ fmol}$  atmospheric neon;  $\pm 1\sigma$ ).

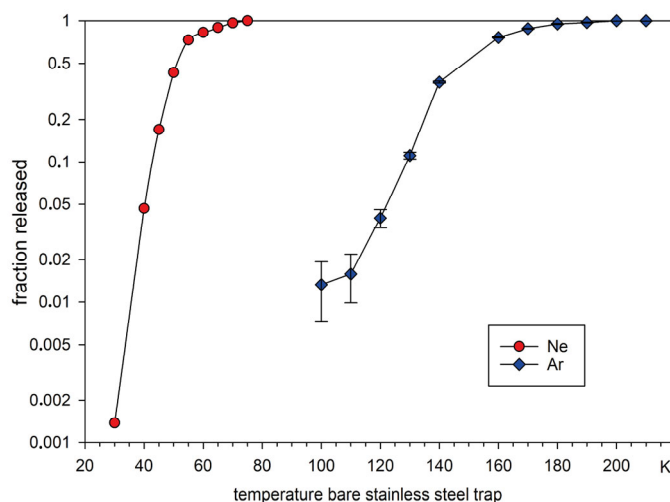
198 iii. Clean-up module ('Sputnik', lab-name, referring to the shape and protrusions of the central  
199 manifold and its faint resemblance to the first satellite, Fig. 1). Arranged around a central  
200 hexagonal 8-port manifold (Kimball Physics, 2.75" spherical hexagon) are the  
201 sample/calibration inlet, the pumping outlet, a pipette leading to a residual gas analyser (Hiden  
202 HAL/3F PIC), two SAES NP50 getters (one operated hot; heating current 1.6 A;  $\sim 300 \text{ }^\circ\text{C}$ ), the  
203 other at room temperature; getters are housed in SAES GP 50 W2F bodies; water cooling is  
204 optional, not used during sample analysis), an optional expansion volume, an internally heated  
205 capacitance manometer (MKS Baratron, Type 628FU5TCF1B; @  $100^\circ\text{C}$ ) and the outlet to the  
206 cryogenic separation unit (Fig. 1). The sample/calibration inlet tubing has an auxiliary port,  
207 which e.g., is used for the crushing extraction module (build around a T4S crushing unit, VU  
208 Amsterdam). The clean-up module is pumped via a manifold connected through gate-valves  
209 (MDC E-GV-1500M-P) to a turbopump (Pfeiffer HiPace 300; backed by a membrane pump,  
210 Pfeiffer MVP 030-3) and an ion pump (Agilent, Vacion 40 plus Starcell).

211 iv. Cryogenic separation module (Fig. 1): Centre of this module is a double-cold trap unit (Janis,  
212 twin coldhead model 204) that has inlet and outlet lines to three traps: a watertrap (operated

213 at 205 K) a bare steel trap ( $\geq 24$  K) and a charcoal trap ( $\geq 10$  K). The cold trap unit is controlled  
214 by a Lakeshore 336 Controller (Cryotronics). This module is pumped by an ion pump (Agilent,  
215 Vacion 40 plus Starcell).

216  
217 The performance of the bare cold trap unit for He, Ne, Ar-separation was calibrated using the  
218 Residual Gas Analyser (Hiden HAL/3F PIC). Neon is quantitatively adsorbed on the bare trap at  
219 24 K (>99.9985 % is adsorbed at 24 K; Fig. 2), in equilibrium about 60% of the helium is adsorbed  
220 at 24 K. We use this to separate helium from neon. Helium is removed (distilled-off in  
221 disequilibrium) either to the ion pump or the 10 K charcoal head, the latter if the He is to be  
222 retained for analysis. Neon is fully released from the bare trap at 80 K, at this temperature argon  
223 is quantitatively retained on the bare trap, permitting quantitative separation of the two gases  
224 (Fig. 2).

225 Besides its functionality to separate noble gases from each other the bare trap serves as coldtrap  
226 during Ne-analysis (held at 80 K) and replaces a liquid nitrogen cooled trap, which would  
227 otherwise customarily be used for this purpose. The latter may introduce intensity fluctuations  
228 during analysis due to changing coolant level, which we avoid with our setup. The last  
229 pneumatically actuated valve before the Helix-Plus MCMS serves as inlet valve, the manual valve  
230 of the Helix-Plus MCMS is permanently open.



231  
232 **Fig. 2: Desorption curves of Ne and Ar on the stainless-steel cold trap measured with the Hiden**  
233 **Quadrupole. The uncertainties of the argon determinations at low fractions released are due to a**  
234 **significant Ar-background of the quadrupole (e.g., measurement at 100 K was just 5% higher than**  
235 **the background).**

### 236 **2.3 Automation**

237 The extraction and purification line can either be operated manually, via a switchboard for the  
238 pneumatic valves and the components' original controllers, or automatically via LabView. Manual

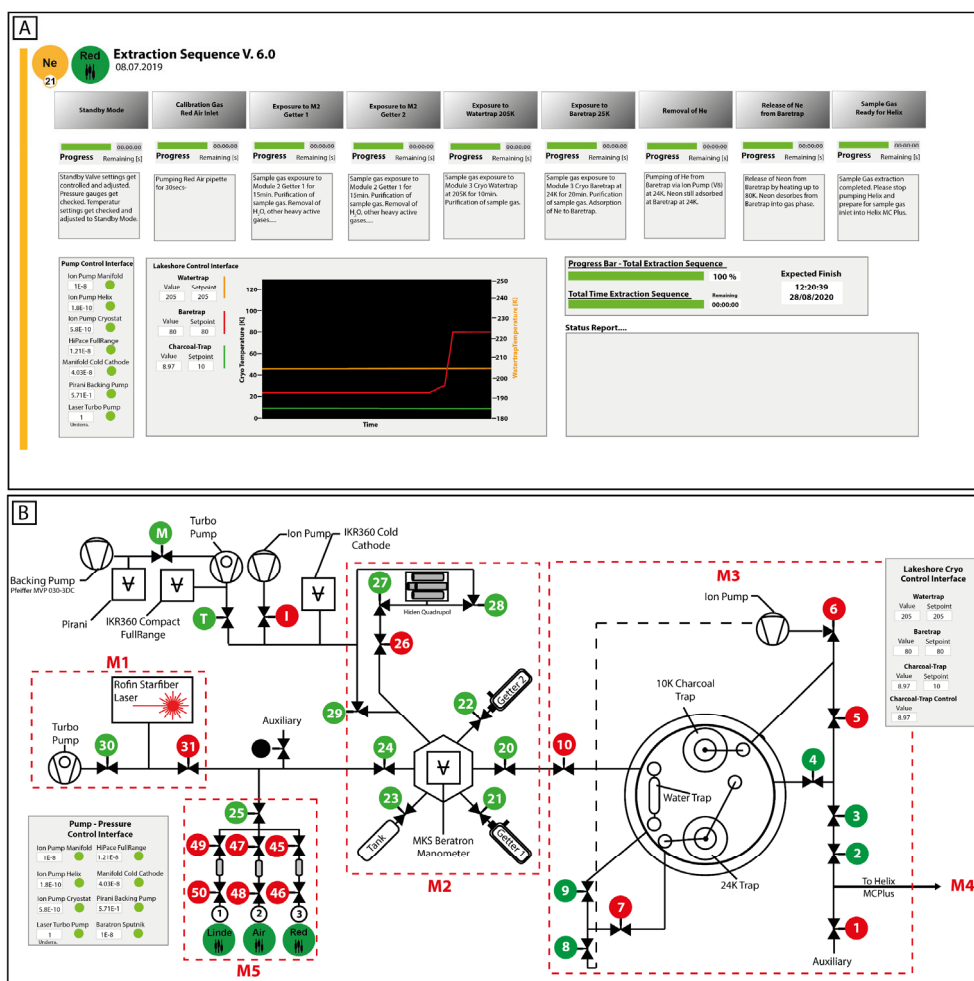


239 operation is mainly used for development of analytical routines, automatic operation generally  
240 for sample and calibration-gas analysis. Automatic operation liberates the operator from  
241 conducting necessarily repetitive tasks, thus helps to prevent mistakes and inconsistencies from  
242 oversight or negligence; it allows to conduct gas purification and separation under precisely  
243 identical conditions. The latter is also assisted by avoiding liquid coolants, which commonly are  
244 affected by variable coolant levels (unless automatically filled with a suitably precise system or an  
245 experienced and conscientious operator). Currently the laser system is operated manually (due  
246 to safety regulations); all subsequent steps - until admission of the gas to the mass spectrometer  
247 - are automated utilizing LabView (Version 2018) in a Windows 10 environment. The mass  
248 spectrometry analysis of the purified gas is conducted with Qtegra (Thermo Fisher Scientific).

249 Valve control electronics were developed and implemented in-house, including digital  
250 input/output modules (I/O modules from National Instruments) and RS-232 communication.  
251 Main devices such as, SAES getter control, Lakeshore Cryo-Controller, turbo and ion pumps  
252 offered already LabView compatible Sub-VI's (Virtual Instrument, **program codes**), which were  
253 implemented into the operation VI (**Fig. 3**). The Agilent Ion Pump Control connection via the  
254 computer interfaces were written/developed in-house.

255 The gauges and controllers of the Turbo pumps (Pfeiffer) and Ion pumps (Agilent) are monitored  
256 via the operation VI (**Fig. 3**). Automatic safety protocols are implemented to protect the extraction  
257 line and equipment against sudden pressure increases. Temperature setting and monitoring of  
258 the three cold traps (Janis Cryostat) is performed by the Lakeshore 336 controller, which in turn  
259 is controlled via the operation VI (**Fig. 3**).

260 LabView computing of the extraction sequence/protocol was programmed in single commands  
261 and steps, joined into command sequences connected in series as sub-VIs for each extraction  
262 protocol (various noble gases and sources of samples or calibration gas). Pressure and  
263 temperature control sequences are programmed in continuous loop to ensure stability and safety  
264 during operation. For handling, a structured user **program interface** was designed (**Fig. 3**), which  
265 provides the user with information about all parameters, total duration, and additionally logs  
266 every extraction step.



267

268 Fig. 3: Screenshots of the operating VI program interface of the Cologne (CGN) Noble Gas Helix  
 269 MCPlus. (A) The Neon VI informs the user in real time about current data, such as pressure and  
 270 temperature, as well as about the current status of the preparation(B) Valve circuit overview. M1-  
 271 M5 indicate the different modules of the extraction line. Valve numbers (1-10,20-31, M, T, I) are  
 272 coloured depending on the current state (green = open, red = closed).

### 273 3. Analytical Procedure

274 Quartz samples are cleaned using standard procedures using dilute HF as etchant (Kohl and  
 275 Nishiizumi, 1992). Up to 600 mg of quartz are loaded into tungsten-cups and covered with a  
 276 tungsten-lid, the latter has a small hole to facilitate gas release. When opening the laser furnace  
 277 for re-loading, the furnace is vented and purged with a continuous flow of pure nitrogen. In normal  
 278 operation, after the initial installation and bake-out, the internal parts of the furnace are never  
 279 again exposed to air. The tungsten cups and lids remain in the nitrogen atmosphere during sample  
 280 (re-)loading. Cups are emptied with a suction micropicker (Micropicker MPC100, VU Amsterdam)  
 281 while seated in the revolver, and weighed samples are transferred from the glass vials into the  
 282 cup through a miniature metal funnel (glass funnels produced undesirable static effects). After  
 283 reloading, the sample revolver is heated by firing the laser on an empty cup; pressure <math>5 \times 10^{-9}</math>

284 mbar is usually achieved after pumping overnight. During this clean-up, and during subsequent  
285 analyses, the temperature of adjacent cups does not exceed 156.6 °C (verified with Indium wire).  
286 Cosmogenic Ne is extracted from quartz by heating the sample with a defocused laser beam at  
287 100 W for 15 min; at these settings, the cup-insides reach ~1200 °C. This temperature allows  
288 reliable extraction of cosmogenic neon (Vermeesch et al., 2015). After heating the furnace, it is  
289 allowed to cool for five minutes before the sample is expanded to the clean-up module.

290 For calibrations, the calibration gas is expanded for 30 sec into the pipette, the pipette volume is  
291 then expanded into the clean-up volume (Fig. 1). After this step, purification is identical for sample  
292 and calibration gases. The pipetting of calibration gas, and the purification of sample and  
293 calibration gases, is fully automatized.

294 Reactive gases are removed by sequential exposure to two metal getters (SAES NP50, Fig. 1); the  
295 first is operated hot, the other at room temperature. The gas is exposed to each for 15 min.  
296 Subsequently the gas is exposed to the water trap at 205 K for 10 min. The remaining inert gases  
297 are exposed to the bare-metal trap at 24 K for 20 min, which is then pumped for 5 min to remove  
298 helium from the sample gas (Fig. 1). The trap is then isolated and heated to 80 K, followed by  
299 five-minutes holding time for re-equilibration. Neon is quantitatively released, and argon is  
300 quantitatively retained on the trap. Subsequently, Ne gas is expanded into the Helix MCMS for  
301 analysis. The bare trap at 80 K remains connected to the mass spectrometer during analysis, for  
302 pumping of CO<sub>2</sub> and Ar evolving from the mass spectrometer.

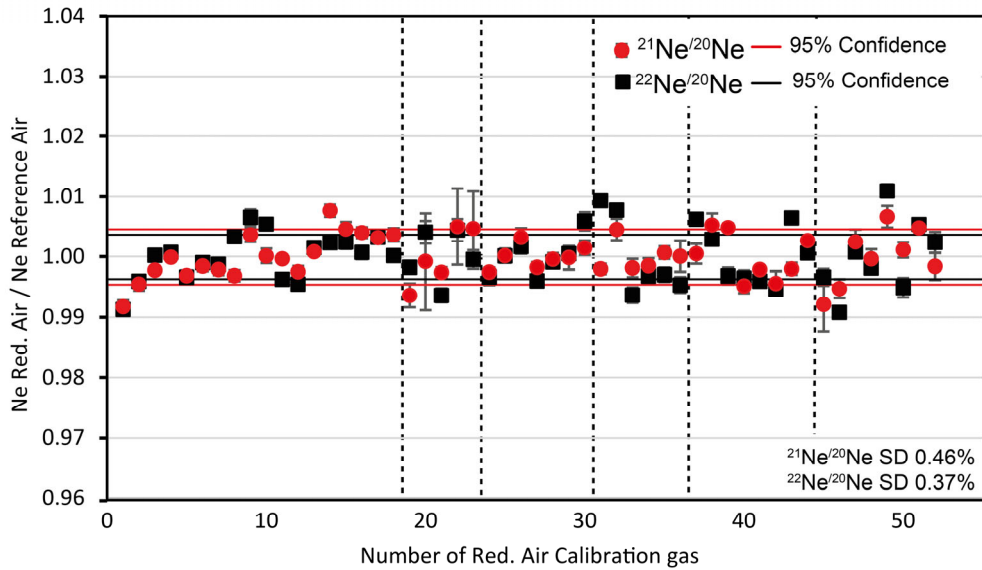
303 The configuration of the Helix is described above. For maximum sensitivity and precision for  
304 abundance determination (Wielandt and Storey, 2019), we use the widest (0.25 mm) source slit  
305 for neon analysis. We run the source at an electron energy of 115 eV, trap current of 200 μA and  
306 an acceleration voltage of 9.9 kV.

307 <sup>20</sup>Ne is measured on the high-resolution L1 Faraday cup (fitted with 10<sup>13</sup> Ω pre-amplifier), fully  
308 resolved from <sup>40</sup>Ar<sup>2+</sup> and from molecular interferences such as HF<sup>+</sup>, H<sub>2</sub><sup>18</sup>O<sup>+</sup>. <sup>21</sup>Ne is measured  
309 off-centre on the high-resolution L1 multiplier, at a position that is free from interference from  
310 <sup>20</sup>NeH<sup>+</sup>. <sup>22</sup>Ne is measured at peak centre on the H1 Faraday cup (fitted with 10<sup>13</sup> Ω pre-amplifier);  
311 interference from CO<sub>2</sub><sup>2+</sup> is corrected via monitoring of the double/single-charged ratio of CO<sub>2</sub>  
312 in-between samples and measurement of CO<sub>2</sub> during sample analysis, which we found to be stable  
313 at 0.0437 ± 0.001 for our system throughout the period for which the data we report here were  
314 obtained. The corresponding corrections of <sup>22</sup>Ne intensities are < 0.3 % for one shot of 'RedAir'  
315 calibration gas (~17 fmol <sup>22</sup>Ne). The uncertainties of the correction are ~2 %, which add < 0.006%  
316 uncertainty to the intensity determinations for 'RedAir'. These values scale linearly for smaller or  
317 larger amounts of <sup>22</sup>Ne as found in samples. CO<sub>2</sub><sup>+</sup> is measured on the Faraday cup of the Axial  
318 collector (fitted with 10<sup>13</sup> Ω pre-amplifier). We refrain from analysing the larger Neon-beams

319 ( $^{22}\text{Ne}$ ,  $^{20}\text{Ne}$ ) on the multipliers, since we found that they are a significant source of  $\text{CO}_2$  upon being  
320 hit by beams larger than those typical for  $^{21}\text{Ne}$  signals (for analysing blanks, however, we use a  
321 multiplier for  $^{20}\text{Ne}$  and  $^{22}\text{Ne}$ ). Besides, the Faraday cups have a superior linearity and stability over  
322 time (Wielandt and Storey, 2019). The mass spectrometer sensitivity, mass-discrimination and  
323 multiplier vs. Faraday gain is calibrated with 'RedAir', which is measured at least once a day during  
324 sample runs. Each batch of samples includes at least one measurement of  $\sim 100$  mg CREU-1  
325 (Vermeesch et al., 2015) to monitor the performance of the extraction and purification system.  
326 We are in the process of producing a new intercomparison material to replace CREU-1, whose  
327 supplies are limited and eventually will run too low for regular use.

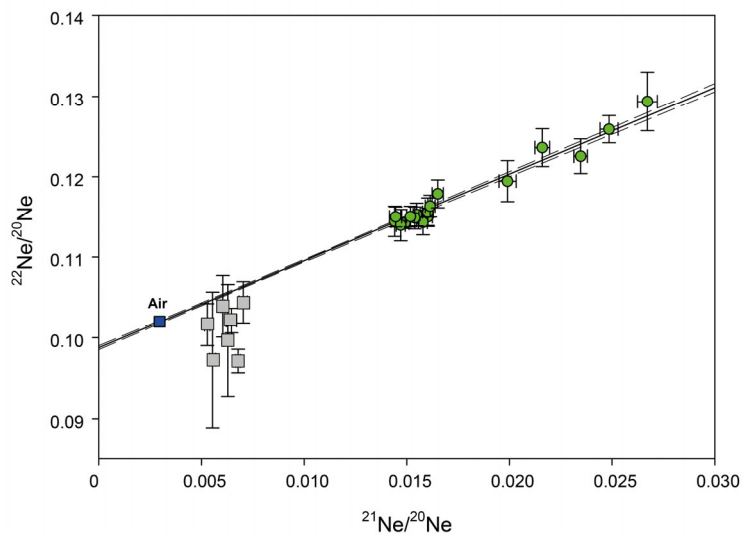
#### 328 **4. Performance**

329 The within-run reproducibility of Neon-isotope ratios as determined for calibration gas ('RedAir',  
330  $\sim 17$  fmol atmospheric Ne) is similar for  $^{21}\text{Ne}/^{20}\text{Ne}$  and  $^{22}\text{Ne}/^{20}\text{Ne}$  ratios, with 0.46 % and 0.37 %  
331 ( $\pm 1\sigma$ ,  $n=52$ ), respectively. This dispersion is larger than the uncertainty of individual  
332 measurements (Fig. 4); this feature, and the values for dispersion, are similar to those reported  
333 for other Helix Plus instruments (Honda et al., 2015; Wielandt and Storey, 2019). **The second**  
334 **measurement period, with the increased uncertainties of the  $^{21}\text{Ne}/^{20}\text{Ne}$  ratios, was performed**  
335 **after an extended period of development work for other noble gas isotopes.** We use the means  
336 and the uncertainty of the means of calibrations within runs to calibrate the measurements  
337 samples, i.e., propagate the observed dispersion in calculations of the abundance of cosmogenic  
338  $^{21}\text{Ne}$  in samples. **Derived  $^{21}\text{Ne}/^{20}\text{Ne}$  and  $^{22}\text{Ne}/^{20}\text{Ne}$  ratios of 22 aliquots of CREU-1, including five**  
339 **power step extractions (Table 1), reveal a spallation line of  $1.078 \pm 0.022$  ( $\pm 2\sigma$ ), which is**  
340 **indistinguishable from the published value of  $1.108 \pm 0.014$  ( $\pm 2\sigma$ ; Vermeesch et al., 2015, Fig. 5).**  
341 The calculated cosmogenic  $^{21}\text{Ne}$  abundances from 22 aliquots of CREU-1 (Table 1) all agree within  
342  $2\sigma$  with their arithmetic mean ( $348 \pm 10 \times 10^6$  atoms/g;  $\pm 2\sigma$ ); thus, we may calculate an error-  
343 weighted mean:  $348 \pm 2 \times 10^6$  atoms/g ( $\pm 2\sigma$ ), which is indistinguishable from the published value  
344 ( $348 \pm 10 \times 10^6$  atoms/g; Vermeesch et al., 2015, see Fig. 6). We conclude that the reproducibility  
345 and accuracy of the current set up at the University of Cologne for determining cosmogenic  $^{21}\text{Ne}$   
346 in quartz is similar to or better than those reported for other laboratories worldwide (Vermeesch  
347 et al., 2015, Fig. 6; Farley et al., 2020; Ma et al., 2015).



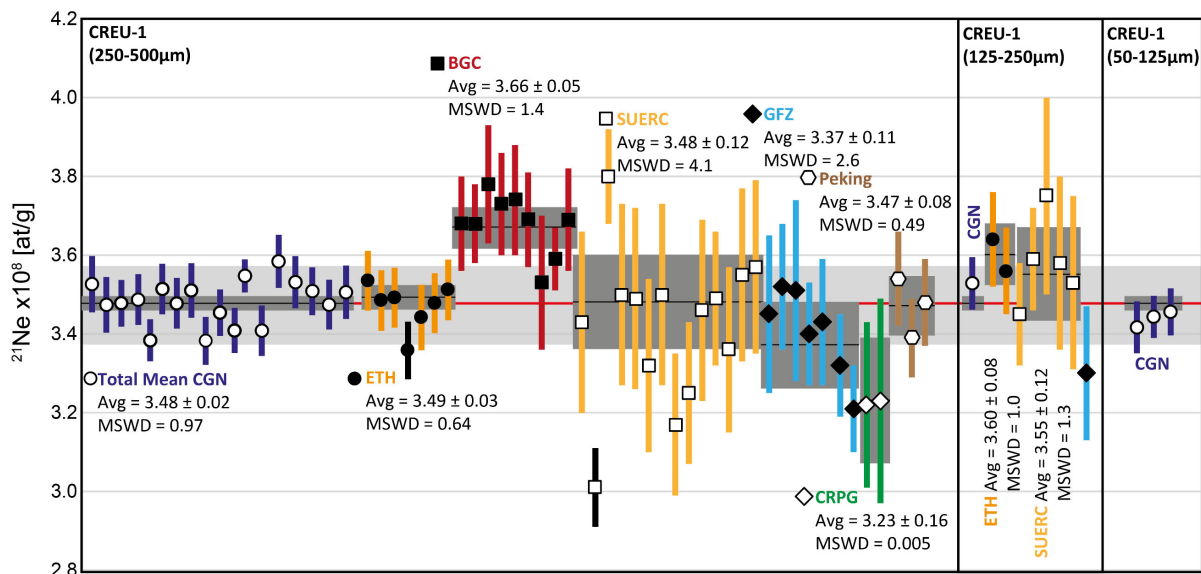
348

349 Fig. 4: Reproducibility of standard gas 'RedAir' measurements for sample runs at CGN noble gas lab,  
 350 during the period between March 2020 and December 2020. Isotopic ratios are normalized to air for  
 351 each run (mean of isotope ratios obtained in run/atmospheric ratio). The larger errors of the  
 352  $^{21}\text{Ne}/^{20}\text{Ne}$ -ratios of the second run may be due to the fact that prior to that run a longer development  
 353 period of other noble gas species, and other sample materials, was conducted. During developmental  
 354 work on a noble gas line, particularly when other gas species are analysed, the residual gas  
 355 composition in the extraction line and in the mass-spectrometer may change. The latter may affect  
 356 the response/stability of multipliers ( $^{21}\text{Ne}$  is the only isotope we measure on the multipliers, thus it is  
 357 the  $^{21}\text{Ne}/^{20}\text{Ne}$  that shows the higher variability). Stippled black lines delineate individual runs. Error  
 358 bars on individual data points are  $\pm 1\sigma$ . Symbol size is commonly larger than the corresponding error  
 359 bars, which may therefore be hidden.



360

361 Fig. 5: Neon-three-isotope plot for CREU-1 intercomparison material measured in Cologne. Error  
 362 bars are  $\pm 1 \sigma$ . The cloud of green symbols displays single-step CREU extractions (100 W-15 min), the  
 363 green dots to the right of the cluster are the initial heating (first extraction of a sample) steps of  
 364 stepwise extractions (at varying laser output), grey rectangles are the subsequent steps that  
 365 invariably had low abundance; for details see Table 1. Data of samples depicted in green are included  
 366 in the regression calculation; data of the grey rectangles are excluded. The slope of the regression of  
 367 the data (forced through air) is  $1.078 \pm 0.022$  ( $\pm 2\sigma$ ), which is indistinguishable from the published  
 368 value of  $1.108 \pm 0.014$  ( $\pm 2\sigma$ ; Vermeesch et al., 2015). The dotted line denotes the 95% confidence  
 369 interval.



370  
 371 Fig. 6: Compilation of CREU-1  $^{21}\text{Ne}$  concentrations ( $\pm 2\sigma$  uncertainties) measured at Cologne (CGN),  
 372 compared to reported  $^{21}\text{Ne}$  concentrations from interlaboratory comparison from Vermeesch et al.  
 373 (2015) and data from the Peking noble gas lab from Ma et al. (2015). Black bars were considered  
 374 outliers by the original authors and not used for calculation of averages (Vermeesch et al., 2015).  
 375 The data is divided into three sections, each for a different CREU-1 grain-size analysed. The average  
 376  $^{21}\text{Ne}$  concentration for CREU-1 of  $3.48 \pm 10 \times 10^8$  at/g reported by Vermeesch et al. (2015) is marked  
 377 as light-grey band and a red line for the mean. Lab-individual error-weighted means are displayed  
 378 as black lines with their respective uncertainty in dark grey. The average obtained for CREU-1 at  
 379 Cologne (all grain-sizes,  $n=22$ ) is  $3.48 \pm 0.02 \times 10^8$  at/g ( $\pm 2 \sigma$ ; error-weighted standard deviation).  
 380 The MSWD values (Mean Square of the Weighted Deviates ('reduced Chi-square', McIntyre et al.  
 381 (1966)) are reported for all individual laboratory-means (Vermeesch et al., 2015; this study). CGN =  
 382 University of Cologne, ETH = Eidgenössische Technische Hochschule Zürich, BGC = Berkeley  
 383 Geochronology Center, SUERC = Scottish Universities Environmental Research Centre Glasgow, CRPG  
 384 = Centre de Recherches Pétrographiques et Géochimiques Nancy, GFZ = Deutsches  
 385 GeoForschungsZentrum Potsdam.

386 Table 1: CREU Data

Sample ID	Mass [g]	Extraction Power [W]	<sup>20</sup> Ne [10 <sup>9</sup> at/g]		<sup>21</sup> Ne/ <sup>20</sup> Ne		<sup>22</sup> Ne/ <sup>20</sup> Ne		<sup>21</sup> Ne* <i>cos.</i> [10 <sup>6</sup> at/g]	
01_CREU1										
250-500μm	0.0997	100	30.97 ± 0.15		0.01434 ± 0.00014		0.11381 ± 0.00129		352.7 ± 3.6	
02_CREU1										
250-500μm	0.0993	100	29.81 ± 0.24		0.01461 ± 0.00015		0.11415 ± 0.00129		347.4 ± 3.5	
03_CREU1										
50-125μm	0.1038	100	24.89 ± 0.15		0.01669 ± 0.00012		0.11646 ± 0.00170		341.7 ± 3.3	
04_CREU1										
50-125μm	0.1319	100	25.73 ± 0.20		0.01634 ± 0.00018		0.11727 ± 0.00089		344.4 ± 2.7	
05_CREU1										
50-125μm	0.1179	100	24.86 ± 0.17		0.01686 ± 0.00017		0.11614 ± 0.00130		345.6 ± 3.0	
06_CREU1										
125-250μm	0.1078	100	27.00 ± 0.35		0.01603 ± 0.00022		0.11499 ± 0.00110		352.9 ± 3.3	
07_CREU1										
250-500μm	0.1210	100	29.13 ± 0.36		0.01490 ± 0.00021		0.11417 ± 0.00065		347.8 ± 3.0	
08_CREU1										
250-500μm	0.1105	100	30.46 ± 0.25		0.01441 ± 0.00018		0.11443 ± 0.00189		348.7 ± 3.2	
09_CREU1										
250-500μm	0.1312	100	26.37 ± 0.32		0.01579 ± 0.00021		0.11428 ± 0.00153		338.4 ± 2.7	
10_CREU1										
250-500μm	0.1128	100	29.92 ± 0.40		0.01470 ± 0.00022		0.11395 ± 0.00195		351.4 ± 3.2	
11_CREU1										
250-500μm	0.1113	100	26.60 ± 0.33		0.01603 ± 0.00026		0.11556 ± 0.00179		347.8 ± 3.2	
12_CREU1										
250-500μm	0.1053	100	30.56 ± 0.36		0.01445 ± 0.00030		0.11498 ± 0.00125		351.1 ± 3.5	
13_CREU1										
250-500μm	0.1125	100	27.01 ± 0.24		0.01548 ± 0.00017		0.11526 ± 0.00143		338.3 ± 3.0	
14_CREU1										
250-500μm	0.1210	100	26.21 ± 0.30		0.01614 ± 0.00024		0.11632 ± 0.00137		345.4 ± 3.0	
15_CREU1										
250-500μm	0.1252	100	25.16 ± 0.19		0.01651 ± 0.00027		0.11786 ± 0.00174		340.9 ± 2.9	
16_CREU1										
250-500μm	0.2063	100	28.54 ± 0.33		0.01539 ± 0.00020		0.11485 ± 0.00137		354.8 ± 2.1	
17_CREU1										
250-500μm	0.1077	100	27.90 ± 0.30		0.01518 ± 0.00019		0.11502 ± 0.00129		340.9 ± 3.2	
18_CREU1										
250-500μm	0.1126	30	16.44 ± 0.16		0.02160 ± 0.00036		0.12362 ± 0.00236			
	0.1126	50	8.61 ± 0.08		0.00628 ± 0.00019		0.09968 ± 0.00692			
	0.1126	70	5.71 ± 0.05		0.00528 ± 0.00013		0.10162 ± 0.00260			
	0.1126	100	3.92 ± 0.05		0.00554 ± 0.00015		0.09727 ± 0.00838		358.5 ± 3.4	
19_CREU1										
250-500μm	0.1111	24	11.96 ± 0.17		0.02672 ± 0.00048		0.12936 ± 0.00364			
	0.1111	100	18.06 ± 0.23		0.00678 ± 0.00012		0.09711 ± 0.00146		353.2 ± 3.3	
20_CREU1										
250-500μm	0.1301	24	14.27 ± 0.12		0.02347 ± 0.00033		0.12255 ± 0.00217			
	0.1301	100	16.51 ± 0.18		0.00646 ± 0.00025		0.10213 ± 0.00152		350.9 ± 3.0	
21_CREU1										
250-500μm	0.1180	30	13.11 ± 0.15		0.02485 ± 0.00044		0.12592 ± 0.00170			
	0.1180	100	14.79 ± 0.09		0.00703 ± 0.00020		0.10440 ± 0.00256		347.5 ± 3.2	
22_CREU1										
250-500μm	0.1075	50	18.42 ± 0.12		0.01991 ± 0.00042		0.11944 ± 0.00256			
	0.1075	100	12.35 ± 0.11		0.00604 ± 0.00010		0.10391 ± 0.00381		350.6 ± 3.4	

387

388 **Conclusion**

389 The performance of the set-up for Neon-isotope measurements in the new noble gas laboratory  
390 at the University Cologne permits state-of-the art analysis of cosmogenic neon. We now regularly

391 perform analysis of samples for cosmogenic neon for our running projects; and are open to new  
392 scientific cooperations.

393 **Author contribution:**

394 TJD, BR, AV **development of the Cologne** noble gas system. TJD, BR performance experiments and  
395 tests. BR, TJD manuscript writing.

396 **Data Availability:**

397 The authors confirm that the data supporting the findings of this study are available within the  
398 article.

399 **Acknowledgements:**

400 The equipment for the noble gas mass spectrometry laboratory described in this paper was  
401 funded by Deutsche Forschungsgemeinschaft (DFG) - project number 259990027 to TJD. The  
402 performance test was conducted and funded in the framework of the Collaborative Research  
403 Center 1211 – Earth Evolution at the Dry Limit, Deutsche Forschungsgemeinschaft (DFG) - project  
404 number 268236062 – SFB 1211. Special thanks go to Dave Wanless for patient training and  
405 continuing support in mastering ‘Aura’. **Furthermore, we want to thank Rainer Wieler and one**  
406 **anonymous reviewer for their constructive feedback on the submitted manuscript.**

407 **Declaration of interest**

408 The authors declare that the research was conducted in the absence of any commercial or financial  
409 relationships that could be construed as a potential conflict of interest.

410 **References**

411 Binnie, S., Reicherter, K., Victor, P., González, G., Binnie, A., Niemann, K., Stuart, F., Lenting, C.,  
412 Heinze, S., Freeman, S., and Dunai, T. J.: The origins and implications of paleochannels in hyperarid,  
413 tectonically active regions: The northern Atacama Desert, Chile, Global and Planetary Change, 185,  
414 103083, doi.org/10.1016/j.gloplacha.2019.103083, 2020.

415

416 Dunai, T. J.: Cosmogenic Nuclides: Principles, concepts and applications in the Earth surface sciences,  
417 Cambridge University Press, doi.org/10.1017/CBO9780511804519, 2010.

418

419 Dunai, T. J., Lopez, G. A. G., and Juez-Larre, J.: Oligocene-Miocene age of aridity in the Atacama  
420 Desert revealed by exposure dating of erosion-sensitive landforms, Geology, 33, 321-324,  
421 doi.org/10.1130/g21184.1, 2005.

422

423 Eberhardt, P., Eugster, O., and Marti, K.: A redetermination of the isotopic composition of  
424 atmospheric neon, Zeitschrift für Naturforschung, 20a, 623-624, doi.org/10.1515/zna-1965-0420,  
425 1965.

426



427 Espanon, V. R., Honda, M., and Chivas, A. R.: Cosmogenic  $^3\text{He}$  and  $^{21}\text{Ne}$  surface exposure dating of  
428 young basalts from Southern Mendoza, Argentina, *Quaternary Geochronology*, 19, 76-86,  
429 doi.org/10.1016/j.quageo.2013.09.002, 2014.  
430

431 Farley, K., Treffkorn, J., and Hamilton, D.: Isobar-free neon isotope measurements of flux-fused  
432 potential reference minerals on a Helix-MC-Plus10K mass spectrometer, *Chemical Geology*, 537,  
433 119487, doi.org/10.1016/j.chemgeo.2020.119487, 2020.  
434

435 Gillen, D., Honda, M., Chivas, A. R., Yatsevich, I., Patterson, D. B., and Carr, P. F.: Cosmogenic  $^{21}\text{Ne}$   
436 exposure dating of young basaltic lava flows from the Newer Volcanic Province, western Victoria,  
437 Australia, *Quaternary Geochronology*, 5, 1-9, doi.org/10.1016/j.quageo.2009.08.004, 2010.  
438

439 Györe, D., Tait, A., Hamilton, D., and Stuart, F. M.: The formation of  $\text{NeH}^+$  in static vacuum mass  
440 spectrometers and re-determination of  $^{21}\text{Ne}/^{20}\text{Ne}$  of air, *Geochimica et Cosmochimica Acta*, 263, 1-  
441 12, doi.org/10.1016/j.gca.2019.07.059, 2019.  
442

443 Honda, M., Zhang, X., Phillips, D., Hamilton, D., Deerberg, M., and Schwieters, J. B.: Redetermination  
444 of the  $^{21}\text{Ne}$  relative abundance of the atmosphere, using a high resolution, multi-collector noble gas  
445 mass spectrometer (HELIX-MC Plus), *International Journal of Mass Spectrometry*, 387, 1-7,  
446 doi.org/10.1016/j.ijms.2015.05.012, 2015.  
447

448 Kohl, C. and Nishiizumi, K.: Chemical isolation of quartz for measurement of in-situ-produced  
449 cosmogenic nuclides, *Geochimica et Cosmochimica Acta*, 56, 3583-3587, doi.org/10.1016/0016-  
450 7037(92)90401-4, 1992.  
451

452 Ma, Y., Wu, Y., Li, D., and Zheng, D.: Analytical procedure of neon measurements on GV 5400 noble  
453 gas mass spectrometer and its evaluation by quartz standard CREU-1, *International Journal of Mass  
454 Spectrometry*, 380, 26-33, doi.org/10.1016/j.ijms.2015.03.004, 2015.  
455

456 Ma, Y., Wu, Y., Li, D., Zheng, D., Zheng, W., Zhang, H., Pang, J., and Wang, Y.: Erosion rate in the  
457 Shapotou area, northwestern China, constrained by in situ-produced cosmogenic  $^{21}\text{Ne}$  in long-  
458 exposed erosional surfaces, *Quaternary Geochronology*, 31, 3-11,  
459 doi.org/10.1016/j.quageo.2015.10.001, 2016.  
460

461 McIntyre, G., Brooks, C., Compston, W., and Turek, A.: The statistical assessment of Rb-Sr isochrons,  
462 *Journal of Geophysical Research*, 71, 5459-5468, doi.org/10.1029/JZ071i022p05459, 1966.  
463

464 McPhillips, D., Hoke, G. D., Liu-Zeng, J., Bierman, P. R., Rood, D. H., and Niedermann, S.: Dating the  
465 incision of the Yangtze River gorge at the First Bend using three-nuclide burial ages, *Geophysical  
466 Research Letters*, 43, 101-110, doi.org/10.1002/2015GL066780, 2016.  
467

468 Niedermann, S.: Cosmic-ray-produced noble gases in terrestrial rocks: dating tools for surface  
469 processes, *Reviews in Mineralogy and Geochemistry*, 47, 731-784, 2002.  
470

471 Niedermann, S., Graf, T., Kim, J., Kohl, C., Marti, K., and Nishiizumi, K.: Cosmic-ray-produced  $^{21}\text{Ne}$  in  
472 terrestrial quartz: the neon inventory of Sierra Nevada quartz separates, *Earth and Planetary Science*  
473 *Letters*, 125, 341-355, doi.org/10.1016/0012-821X(94)90225-9, 1994.  
474

475 Ritter, B., Stuart, F. M., Binnie, S. A., Gerdes, A., Wennrich, V., and Dunai, T. J.: Neogene fluvial  
476 landscape evolution in the hyperarid core of the Atacama Desert, *Scientific Reports*, 8, 13952,  
477 10.1038/s41598-018-32339-9, 2018.  
478

479 Saxton, J.: The  $^{21}\text{Ne}/^{20}\text{Ne}$  ratio of atmospheric neon, *Journal of Analytical Atomic Spectrometry*,  
480 35, 943-952, DOI: 10.1039/DOJA00031K 2020.  
481

482 Vermeesch, P., Balco, G., Blard, P. H., Dunai, T. J., Kober, F., Niedermann, S., Shuster, D. L., Strasky, S.,  
483 Stuart, F. M., Wieler, R., and Zimmermann, L.: Interlaboratory comparison of cosmogenic  $\text{Ne-21}$  in  
484 quartz, *Quaternary Geochronology*, 26, 20-28, doi.org/10.1016/j.quageo.2012.11.009, 2015.  
485

486 Wielandt, D. and Storey, M.: A new high precision determination of the atmospheric  $^{21}\text{Ne}$   
487 abundance, *Journal of Analytical Atomic Spectrometry*, 34, 535-549, doi.org/10.1039/C8JA00336J,  
488 2019.  
489